Structural Basis of UDP-galactose Binding by α-1,3-Galactosyltransferase (α3GT): Role of Negative Charge on Aspartic Acid 316 in Structure and Activity[†]

Percy Tumbale,[‡,§] Haryati Jamaluddin,[‡,||,⊥] Nethaji Thiyagarajan,[||] Keith Brew,*,[§] and K. Ravi Acharya*,[||]

Department of Biomedical Science, Florida Atlantic University, 777 Glades Road, Boca Raton, Florida 33431, and Department of Biology and Biochemistry, University of Bath, Claverton Down, Bath BA2 7AY, U.K.

Received May 9, 2008; Revised Manuscript Received June 20, 2008

ABSTRACT: α-1,3-Galactosyltransferase (α3GT) catalyzes the transfer of galactose from UDP-galactose to form an α 1−3 link with β-linked galactosides; it is part of a family of homologous retaining glycosyltransferases that includes the histo-blood group A and B glycosyltransferases, Forssman glycolipid synthase, iGb3 synthase, and some uncharacterized prokaryotic glycosyltransferases. In mammals, the presence or absence of active forms of these enzymes results in antigenic differences between individuals and species that modulate the interplay between the immune system and pathogens. The catalytic mechanism of α3GT is controversial, but the structure of an enzyme complex with the donor substrate could illuminate both this and the basis of donor substrate specificity. We report here the structure of the complex of a low-activity mutant α3GT with UDP-galactose (UDP-gal) exhibiting a bent configuration stabilized by interactions of the galactose with multiple residues in the enzyme including those in a highly conserved region (His315 to Ser318). Analysis of the properties of mutants containing substitutions for these residues shows that catalytic activity is strongly affected by His315 and Asp316. The negative charge of Asp316 is crucial for catalytic activity, and structural studies of two mutants show that its interaction with Arg202 is needed for an active site structure that facilitates the binding of UDP-gal in a catalytically competent conformation.

Glycoconjugates, specifically glycoproteins and glycolipids, are important glycoproteins and glycolipids, are important components of cell surfaces and the extracellular environment that mediate cellular and molecular interactions. They influence the structures and the physical and functional properties of macromolecules (*1*). Defects in glycosylation are associated with human diseases (*2*) while the ability of glycans to modulate immune responses leads to them playing a critical role in susceptibility and resistance to pathogens (*3, 4*).

The structures of the glycan moieties of glycoconjugates depend on the specificity of glycosyltransferases (GTs),[1] the enzymes that catalyze their synthesis. GTs catalyze the transfer of a sugar residue from activated donor molecules (e.g., UDP-galactose) to a defined reactive group on a specific acceptor molecule, forming a glycosidic bond (*5*). GTs are specific for the glycosyl donor, the acceptor substrate, and for the glycosidic linkage in the product. Since their

specificities determine the structures of oligomers that contain high levels of biological information, an understanding of the structural basis of their specificity and catalytic activities is a core issue in the field of glycobiology.

UDP-galactose β-galactosyl α-1,3-galactosyltransferase (α3GT, EC 2.4.1.151), a member of glycosyltransferase family 6 of the CAZY database (*6*), is a retaining GT that catalyzes the transfer of galactose from UDP-α-D-galactose into an α-1,3 linkage with β-galactosyl groups in glycoconjugates (*7*). Its homologues include the histo-blood group A and B glycosyltransferases, Forssman glycolipid synthase, iGb3 synthase, and several mammalian, bacterial, and viral proteins of unknown function. α3GT and its products are present in most mammals, but active forms of the enzyme are not produced by old world primates including humans (*8*) because of inactivating mutations (*8, 9*). The lack of its products, collectively designated the α-Gal epitope, results, in these species, in the production of natural antibodies directed toward them. Such antibodies represent a defense against infection by pathogenic microorganisms and viruses (*10*) but are also a barrier to xenotransplantation of organs from species that have active forms of α3GT (*11–13*).

In previous studies, structures have been determined for wild-type α3GT and various mutants, in the free state and in complexes with substrates and inhibitors (*14–17*). Structures of wild-type α3GT cocrystallized with UDP-galactose (UDP-gal) were found to contain UDP and galactose, reflecting the relatively high UDP-gal hydrolase activity of α3GT. Recently, we reported the structure of an inhibitory analogue of UDP-gal, UDP-2F-galactose (UDP-2F-gal), and

Mn^{2+} in a complex with a variant of α3GT that contains a conservative mutation in the C-terminal region, Arg365Lys (*18*). To identify residues involved in donor substrate binding and specificity, we have determined the structure of a complex of the donor substrate UDP-gal with a previously characterized mutant of α3GT (Glu317Gln) that has negligible galactosyltransferase and UDP-galactose hydrolase activities (*16*). The complex contains an intact substrate in a well-defined bent shape and displays a unique structure for the C-terminal region of α3GT and identifies interactions between the enzyme and substrate whose roles have been investigated by mutagenesis. These observations provide a detailed insight into the structural basis of donor substrate specificity in α3GT.

EXPERIMENTAL PROCEDURES

Expression, Mutagenesis, and Enzyme Activity Measurements. Mutants of the catalytic domain of α3GT were constructed using the PCR megaprimer method. The proteins were purified as described previously (*19*). Activity measurements and steady-state kinetic measurements were performed as previously reported (*19*).

X-ray Crystallography. The purified bovine α3GT mutants were stored at −20 °C in 20 mM MES−NaOH buffer (pH 6) containing 50% glycerol. Crystals of the Glu317Gln mutant in complex with UDP-gal were grown at 16 °C by the vapor diffusion, hanging drop method by mixing 1 μL of the protein at 5 mg/mL in 20 mM MES−NaOH buffer, pH 6.0, and 10% glycerol, containing 10 mM $MnCl_2$ and 10 mM UDP-gal, with an equal volume of reservoir solution containing 10% PEG 6000, 0.1 M Tris-HCl, pH 8.0, and 8% MPD, respectively. Crystals of the Asp316Glu and Asp316Asn mutants were grown in the presence of UDP-gal and *N*-acetyllactosamine under conditions containing 5−10% PEG 6000, 0.1 M Tris-HCl, pH 8.0, and 5−14% MPD by mixing 1 μL of the protein at 5 mg/mL in the presence of 10 mM UDP-Gal, 10 mM $MnCl_2$ and 10 mM *N*-acetyllactosamine with an equal volume of the reservoir solution. Before data collection the crystals were flash-cooled at 100 K in a cryoprotectant containing the reservoir solution and 25% glycerol. Diffraction data from single crystals were collected on stations 14.2/10.1 of the Synchrotron Radiation Source (Daresbury, U.K.), each of which was equipped with a Quantum-4 CCD detector (Area Detector Systems Corp.). A total of three data sets were collected: the Glu317Gln mutant in complex with UDP-gal, the Asp316Glu mutant in complex with UDP-gal and *N*-acetyllactosamine, and the Asp316Asn mutant in complex with UDP-gal and *N*-acetyllactosamine at 1.82, 1.76, and 2.2 Å, respectively. Raw data images were indexed and scaled using DENZO and SCALEPACK modules of the HKL suite (*20*).

The structures of all α3GT mutant complexes were determined by the molecular replacement method using the native form II structure [PDB code 1K4V (*14*)] as a search model with the program MOLREP (*21*). Crystallographic refinement was performed using the program package CNS (*22*) or REFMAC (*23*). After the initial refinement, the difference electron density maps revealed the presence of all the mutated residues at their respective positions and a UDP-gal and Mn^{2+} ion bound to the Glu317Gln mutant, UDP, Mn^{2+} and *N*-acetyllactosamine bound to the Asp316Glu

and Asp316Asn mutants. Several rounds of energy minimization, simulated annealing, individual *B*-factor refinement, and model building using the program COOT (*24*) were performed until the R_{free} could not be improved. Water molecules were gradually included into the model at positions corresponding to peaks in the $|F_o| - |F_c|$ electron density map with heights greater than 3σ and at H-bond distance from appropriate atoms. Residues with poor side-chain density were modeled as alanines, and regions with very poor main chain electron density were excluded from refinement so as not to bias the model. Refinement was carried out until the R_{cryst} and R_{free} could not be improved. The data collection processing and the final refinement statistics for the five structures are listed in Table 1.

Protein Data Bank Accession Codes. The atomic coordinates and the structure factors that have been deposited with the RCSB Protein Data Bank are as follows: 2VS5, 2VS4, and 2VS3 for E317Q, D316E, and D316N complexes, respectively.

RESULTS

Crystal Structure of the Glu317Gln Mutant in Complex with UDP-gal. Orthorhombic crystals with two molecules per asymmetric unit were grown for the Glu317Gln mutant in the presence of UDP-gal and Mn^{2+}. As observed previously for the Glu317Gln mutant in its complex with UDP and lactose (*16*), the mutation produces no overall change in conformation (root-mean-square deviation of 0.52 Å for C^α atoms between the mutant and wild-type structures). The glutamate to glutamine mutation is sterically conservative and produced no change in the electron density. The structure of this complex contrasts with the previously determined structure of wild-type α3GT in a complex with UDP-gal in which the galactose moiety was cleaved from the UDP as β-galactose and had rearranged at a distance of approximately 4 Å from the β-phosphate of UDP (*15*). In the structure of the Glu317Gln complex, an intact UDP-gal is bound in the active site of each of the two molecules (Figure 1A), reflecting the low hydrolase activity of the mutant relative to wild-type α3GT (*16*). UDP-gal binds to the enzyme in a bent conformation that resembles that of the inhibitor, UDP-2F-gal in its complex with the Arg365Lys mutant of α3GT (*18*). The galactose moiety is almost perpendicular to the plane of the diphosphate moiety of the UDP whereas the UDP moiety binds essentially in the same manner as the UDP component in the complexes of wild-type and mutant α3GTs with UDP (*14–17, 25*). Contacts between the protein and the UDP moiety are the same as in these earlier complexes, except for those involving residues in the C-terminal region. The α-galactosyl moiety of the intact UDP-gal is highly ordered within the active site of the Glu317Gln mutant as shown by its well-defined electron density (Figure 1B). The ring adopts a stable $^4C_1$ chair conformation and forms hydrogen bonds with the side-chain atoms of residues Arg202, Asp225, His280, Ala 281, His315, Asp316, and Gln317. Both O2′ and O3′ hydrogen bond with the side-chain carboxylate of Asp225 while O3′ and O4′ hydrogen bond with the carboxylate of Asp316 (Figure 1C, Table 2); this suggests that both aspartates have important roles in donor substrate binding and catalysis. Interestingly, Asp225 is invariant in the entire α3GT family while Asp316 is conserved in all except in Forssman glycolipid synthase, where

Table 1: Crystallographic Data Processing and Refinement Statistics

proteins	E^{317}Q mutant	D^{316}E mutant	D^{316}N mutant
ligands used in crystallization	10 mM UDP-gal 10 mM Mn^{2+}	10 mM UDP-gal 10 mM Mn^{2+} 10 mM *N*-acetyllactosamine	10 mM UDP-gal 10 mM Mn^{2+} 10 mM *N*-acetyllactosamine
ligands observed in crystal structure	Mn^{2+} UDP-gal	Mn^{2+} UDP *N*-acetyllactosamine	Mn^{2+} UDP *N*-acetyllactosamine
disordered regions	C-terminus (358−368) except for Arg^{365}		
space group	*P*2$_1$2$_1$2$_1$	*P*2$_1$	*P*2$_1$
no. of molecules/asymmetric unit	2	2	2
crystal parameters			
a (Å), *b* (Å), *c* (Å)	87.03, 91.38, 94.63	45.25, 94.63, 94.69	45.12, 94.38, 94.94
α (deg), β (deg), γ (deg)	90.0, 90.0, 90.0	90.0, 98.9, 90.0	90.0, 99.3, 90.0
resolution (Å)	1.82	1.77	2.2
R_{symm} (%)[a] (outermost shell)[b]	10.1 (51.7)	7.2 (22.6)	12.0 (30.6)
completeness (%) (outermost shell)[b]	97.9 (97.9)	92.3 (87.5)	94.9 (86.2)
$I/\sigma I$ (outermost shell)[b]	7.8 (2.5)	20.4 (3.6)	9.7 (2.5)
total reflections	808570	412471	353562
unique reflections	68394	76955	39855
R_{cryst}[c]/R_{free}[d] (%)	18.7/20.1	18.3/21.0	18.3/22.7
Ramachandran plot			
% core/allowed	89.5/10.5	87.8/12.2	90.5/9.5
RMSD from ideal			
bond angles (deg)	1.481	1.422	1.085
bond lengths (Å)	0.015	0.007	0.009
no. of water molecules	723	1256	426

[a] $R_{symm} = \sum_h\sum_i[|I_i(h) - \langle I(h)\rangle|/\sum_h\sum_iI_i(h)]$, where I_i is the *i*th measurement and $\langle I(h)\rangle$ is the weighted mean of all measurements of $I(h)$. [b] Figures in parentheses refer to the outermost shell (1.89−1.82, 1.83−1.77, and 2.26−2.20 Å for Glu317Gln, Asp316Glu, and Asp316Asn ligand complexes, respectively). [c] $R_{cryst} = \sum_h|F_o - F_c|/\sum_hF_o$, where F_o and F_c are the observed and calculated structure factor amplitudes of reflection *h*, respectively. [d] R_{free} is equal to R_{cryst} for a randomly selected 5% subset of reflections not used in the refinement.

it is replaced by Glu. Bidentate hydrogen bonding with monosaccharide −OH groups has also been observed in other glycosyltransferases including the retaining galactosyltransferase, LgtC, from *Neisseria meningitides* (*26*), cyclodextrin glycosyltransferases, and α-amylases (*27*). The main-chain nitrogen atom of the mutated residue, Gln317, is at an ideal hydrogen bond distance (3.3 Å) from O4′ of the galactose moiety, but the side chain does not H-bond with the UDP-gal and is positioned as if it is stacking with the galactosyl ring (Figure 1A). A water molecule interacts directly with the α-galactosyl moiety of UDP-gal, making bidentate interactions with O6′ and O5′ of galactose (in addition to the ND1 atom of His315 with O6′) and with O1B of the β-phosphate of UDP. In the previously determined structure of the Arg365Lys mutant in complex with UDP-2F-gal no water molecule is present that corresponds to that in the UDP-gal complex. This might reflect differences in interactions of the enzyme with an inhibitor and a substrate or an indirect effect of the Arg365Lys mutation arising from the conformation of the C-terminal region (*18*).

Previous studies of α3GT have shown that the binding of UDP or UDP-2F-gal induces structural changes in two regions of the protein, a loop centered around Trp195 and the C-terminal 11 residues (*14, 15, 18*). In this context, it is particularly interesting that the C-terminal region (residues 358−368) is largely disordered in the UDP-gal complex, with the exception of Arg365, a residue that is conserved in all known homologues of α3GT. The electron density of the side chain of Arg365 is well defined, but there is essentially no electron density for the remainder of the C-terminal region (Figure 1B). The side chain of Arg365 interacts directly with the α-phosphate of the UDP moiety, as in the structure of the UDP complex of wild-type α3GT. The source of the difference in the interactions between the C-terminal region of this complex and those in the UDP complex of the wild-type enzyme appears to be the absence of interactions with

the network of water molecules surrounding the β-phosphate of UDP which is present in the UDP complex but absent from the UDP-gal complex. This results from the displacement of the solvent network by the α-galactosyl component of UDP-gal. In the UDP complex, interactions of the Arg365 side chain and the α-phosphate of UDP with these solvent molecules stabilize the closed conformation in which the C-terminus covers the active site. The fact that only the side chain of Arg365 interacts with the intact UDP-gal, while other residues of the C-terminus are disordered, supports previous mutational studies that emphasize the importance of Arg365 in catalysis (*14*). In the previously characterized complex of the Arg365Lys mutant with UDP-2F-gal, Thr358 and Lys359 are ordered but residues 360−368 are disordered; comparison with the present structure suggests that the disorder in residue 365 in that structure may reflect the mutation of Arg365 to Lys.

Properties of Catalytic Site Mutants. The structure of the UDP-gal complex shows that Arg202, Asp225, His280, Ala281, Ala282, and residues 314 to 317 are proximal to the galactosyl component of the donor substrate (Figure 1C, Table 2). The roles of some of these residues have been previously investigated by mutagenesis. Thus, the mutation of Asp225 to Asn was found to abrogate catalytic activity (*19*), and the mutation of His280 to an array of residues was found to reduce activity to <1% of wild-type, except that the Gln mutation which reduced k_{cat} 9-fold and increased the K_m and K_i for UDP-gal (*23*). The region corresponding to residues 314−317 of α3GT is highly conserved in both eukaryotic and prokaryotic homologues of α3GT except for a group of mammalian proteins that do not appear to be functional glycosyltransferases. Glu317 and Ser318 are invariant, while His315 and Asp316 are replaced only in Forssman glycolipid synthase by Gln or Arg and Glu, respectively. The residue corresponding to Trp314 is Val in
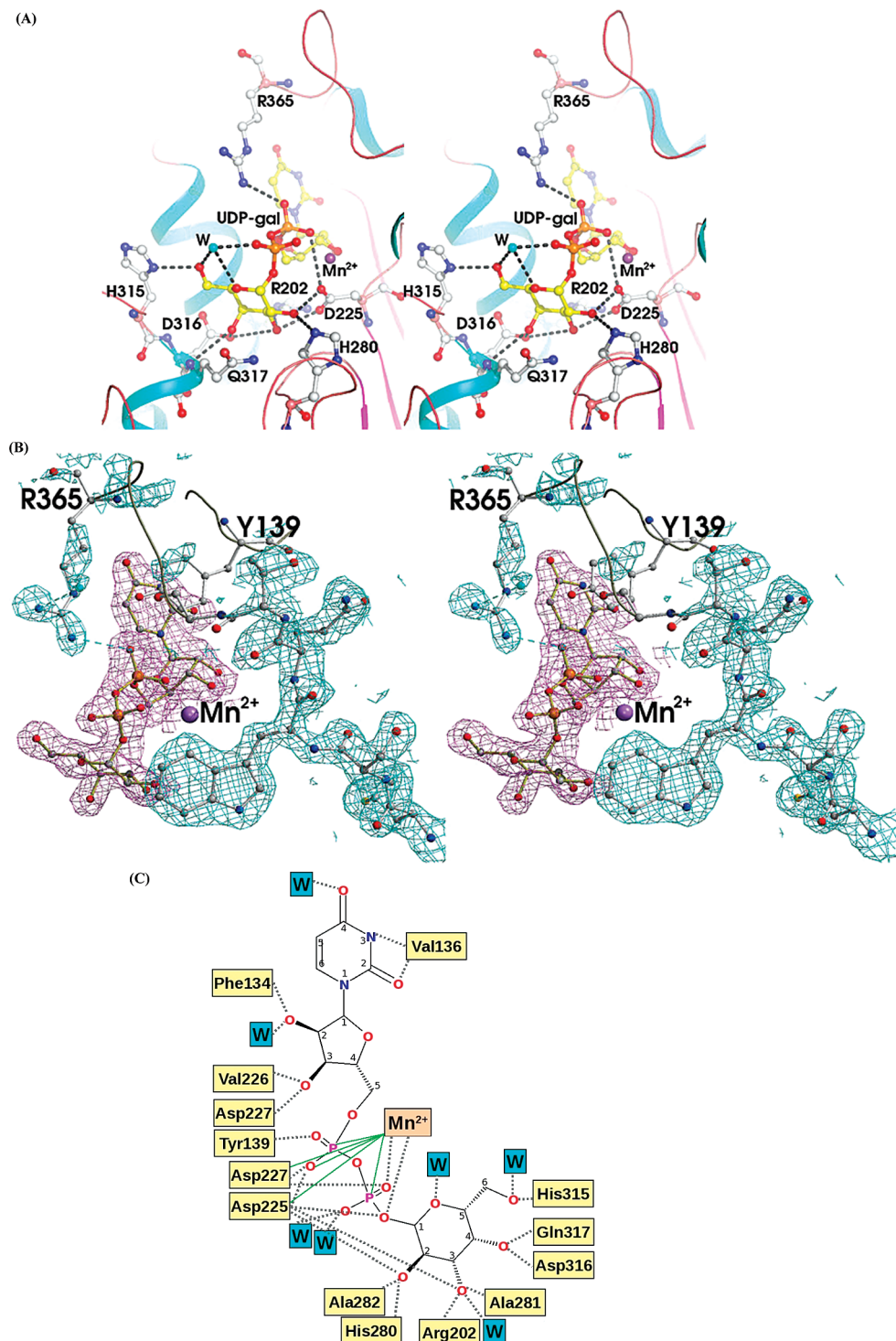
FIGURE 1: (A) Close-up view of the active site interactions of the galactose moiety of UDP-gal with the surrounding residues. Also shown are the Mn^{2+} ion and a water molecule which interacts directly with the sugar. The UDP-gal molecule is shown in yellow, Mn^{2+} ion as a purple-violet sphere, and water molecule as a blue sphere. Residues from the active site cleft and from the C-terminus are represented as ball-and-stick model with standard colors for the atoms. Close interactions are displayed as black dashed lines. (B) The C-terminal region (with standard colors for the atoms) of the Glu317Gln mutant in complex with UDP-gal. Shown is the disordered and broken electron density for the C-terminal region compared to the rest of the enzyme in cyan color and the ordered UDP-gal in pink color. The electron density ($2F_o - F_c$ map) is contoured at 1.0σ. (C) A diagram showing the main contact residues for the Glu317Gln mutant with the donor UDP-gal. Hydrogen bonds are shown as dashed lines, and the coordinating residues with Mn^{2+} ion are displayed as green lines. Bound water molecules are denoted by the letter "W". The figure was created using the programs PyMOL (http://www.delanoscientific.com) and BOBSCRIPT (*34*).

some prokaryotic enzymes while His318 is replaced by Tyr and even Leu in some homologues. Previous mutational studies of residues in this region have shown that the substitution of Tyr for Trp314 reduces k_{cat} for the galacto-syltransferase reaction 30-fold (*17*) while the mutation of

Glu317 to Gln (the mutant used in the present structural study) lowered catalytic activity 2000-fold and increased K_m for acceptor substrates (*16*). Here we have investigated the effects of substitutions for other residues in this region (Table 3). Gln and Arg were substituted for His315, based on the

Table 2: Hydrogen Bond Interactions between the Gal Portion of UDP-gal and the α3GT Glu317Gln Mutant

ligand atom of Gal of UDP-gal	interacting atoms (α3GT-Glu317Gln)	distance (Å)
O2′	OD2 225 Asp	2.79
	NE2 280 His	3.08
	N 282 Ala	3.36
O3′	OD1 225 Asp	3.02
	water	3.09
	NH2 202 Arg	2.78
	O 281 Ala	2.93
O4′	OD2 316 Asp	2.77
	N 317 Gln	3.22
O6′	ND1 315 His	2.88
O5′	water	3.49
O6′		2.67
O1B		2.90

Table 3: Effects of Mutations on the Catalytic Properties of α3GT

enzyme	k_{cat}	K_a	K_b	K_{ia}
WT	6.4	0.43	20	0.14
H315R	0.014	0.10	31	ND[a]
H315Q	3.23	1.83	25	0.08
D316E	2.48	0.16	6.4	0.06
D316N	inactive[b]			
S318A	3.1	1.33	39	0.56
H319A	3.5	0.22	19	ND[a]
H319E	inactive[b]			
H319Y	inactive[b]			

[a] ND, not determined. [b] The activity is too low to accurately characterize even at relatively high concentrations of enzyme. We estimate that it is more than 10000-fold lower than wild-type.
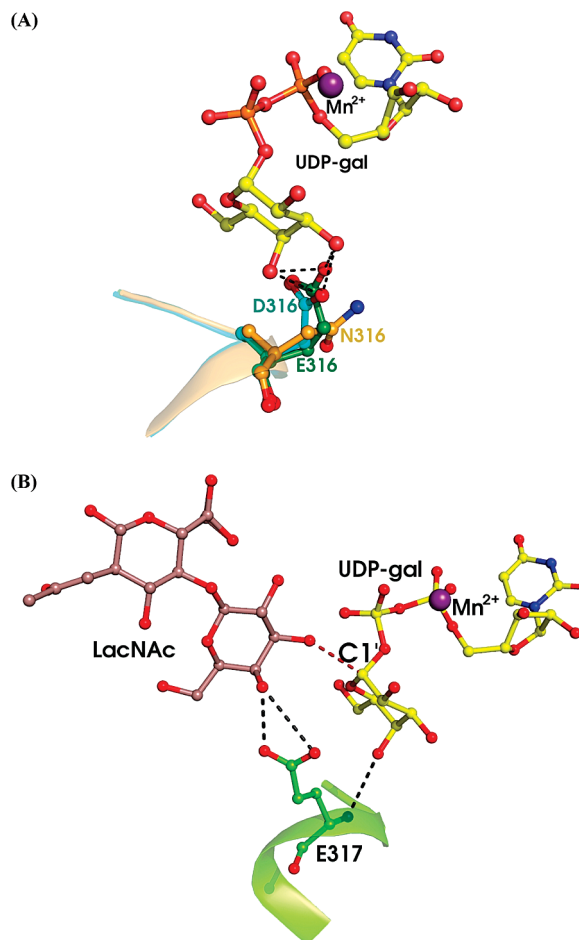

FIGURE 2: (A) Superposition of the Glu317Gln mutant structure in complex with UDP-gal with the Asp316Glu and Asp316Asn structures. (B) Structure of the wild-type α3GT in complex with LacNAc (PDB code 1GX4; ref *15*) modeled with UDP-gal from the Glu317Gln structure. The red dashed line shows the distance between LacNAc and C1′ of UDP-gal, which is approximately 2.53 Å. The figure was created using the program PyMOL (http://www.delanoscientific.com).

residues found at this site in Forssman glycolipid synthase from different species. The substitution of Gln produced modest changes in kinetic parameters for lactose whereas the Arg substitution led to a major loss of catalytic activity arising from an ~500-fold reduction in k_{cat}. It is interesting that Arg is present at this site in human Forssman glycolipid synthase, in contrast to Gln in most other species; it seems likely that this substitution contributes to the lack of Forssman synthase activity and Forssman antigen in human tissues (*28*). Two conservative substitutions were made for Asp316, to Asn and Glu. As shown in Table 3, the Asn mutation shows that negative charge on this residue is crucial for catalytic activity while the increased side-chain size (Glu) produces relatively modest reductions in k_{cat} and the K_m for lactose. Ser318 and His319 are more distant from UDP-gal in its complex with Glu317Gln (Figure 1A); alanine mutagenesis indicates that Ser318 is functionally more important than His319 as reflected in a 10-fold vs 2-fold reduction in k_{cat} (Table 3). This may reflect the proximity of Ser318 to Glu317, which has a key role in catalytic activity. Other substitutions for His319 that produce a change in charge (Glu) and size (Tyr) resulted in a complete loss of activity.

Structures of the Asp316Glu and Asp316Asn Mutants in Complex with UDP and N-Acetyllactosamine. Because of their contrasting effects on catalytic activity, we investigated the structures of the mutants with Asn and Glu substitutions for Asp316. Monoclinic crystals with two molecules per asymmetric unit were grown in the presence of UDP-gal, Mn²⁺, and *N*-acetyllactosamine. However, electron density is only observed for the UDP moiety of the UDP-gal, suggesting that the galactose moiety has been lost through transfer to *N*-acetyllactosamine during crystallization. The possibility that the sugar moiety is present but disordered because of the mutation is unlikely in the case of the Asp316Glu mutant because of its high level of catalytic activity. The "closed" conformation of the C-terminal region in both structures is also typical of UDP-containing complexes of wild-type α3GT, and it is reasonable to conclude that these structures represent dead-end inhibitory complexes containing UDP and acceptor substrate. The binding of UDP in both structures is almost identical to that in the wild-type enzyme in its complex with UDP. The binding of the acceptor substrate, *N*-acetyllactosamine, is also essentially the same as in the wild-type complex with a slight perturbation in the orientation of the *N*-acetylglucosamine moiety. The region around the active site is similar to that of wild-type α3GT except for the site of the mutation. While the orientation of Glu316 in the Asp316Glu mutant is essentially the same as the Asp316 in the wild-type structure (see Figure 2A), in contrast, Asn316 in the Asp316Asn mutant has undergone large change in orientation resulting in a 180° turn from the position of the Asp side chain in the wild-type enzyme (Figure 2A). This would be expected to disrupt interactions with the galactosyl moiety of UDP-gal and is likely to contribute to the essentially undetectable catalytic activity of this mutant.

Table 4: Comparison of Interactions of UDP-gal and UDP-2F-gal with
α3GT in Different Complexes

residue [atom]	UDP-gal	UDP-2F-gal	UDP + β-Gal
S199 [OD]	none	none	O1′, O5′
R202 [NH2]	O3′	O3′	O6′
D225 [OD1]	O3′	O3′	O6′
D225 [OD2]	O2′	F2′, O3′	O6′
H280 [NE2]	O2′	F2′	none
A281 [N]	O3′	none	none
A282 [O]	O2′	none	none
W314 [O]	none	none	O3′, O4′
H315 [ND1]	O6′	O6′	O2′
D316 [OD1]	none	O4′	none
D316 [OD2]	O4′	O4′	none
E317 or Q317 [N]	O4′	O4′	O4′
WAT	O5′, O6′, O1B, O3′	none	O2′

DISCUSSION

It is interesting to compare the enzyme-UDP-gal complex
reported here with the previously described structure of the
complex of α3GT with the inhibitor, UDP-2F-gal (*18*), and
also with the complex containing the products of UDP-gal
hydrolysis, UDP and β-galactose (*15*), although the UDP-
gal and UDP-2F-gal complexes contain α3GT mutants with
substitutions at different locations in the active site. UDP-
gal interacts with a similar group of residues as the inhibitor
UDP-2F-gal, but there are distinct differences both in
enzyme−ligand contacts and in enzyme structure between
the complexes. Table 4 compares enzyme−ligand H-bonds
in the three complexes. The UDP-gal and UDP-2F-gal are
bound in similar "bent" conformations echoing the structures
of donor substrate−enzyme complex structures of some other
retaining glycosyltransferases particularly LgtC (*26*) and
Waag (*29*). This suggests that binding the donor substrate
in this type of conformation may be a shared feature in their
catalytic mechanisms. A recent NMR study of UDP-hexose
interactions with the blood group B galactosyltransferase
suggests that, in this homologue of α3GT, UDP-galactose
and the nonsubstrate, UDP-glucose, are both bound in a
similarly folded-back conformation; they suggest that the
inability of Asp302 (corresponding to Asp316 of α3GT) to
interact with the 4-OH of the glucose of UDP-glc may be a
key to specificity of the blood group B enzyme for UDP-gal
(*30*). It is possible that the situation differs between that
enzyme and α3GT even though they are homologous;
inspection of a modeled enzyme complex with UDP-glc
indicates that clashes between the 4-OH of the glucose and
the side chain of Arg202 are likely to prevent UDP-glc from
binding in the bent conformation observed for UDP-gal,
suggesting that this residue is important for donor substrate
specificity.

Interestingly, there are significant differences in H-bonding
interactions between 2F-gal of UDP-2F-gal with the enzyme
relative to those between the galactose of UDP-gal and
enzyme in their respective complexes. Specifically, H-bond
interactions are present in the 2F-gal complex between the
second carboxylate oxygen of Asp316 and O3′ and O4′, and
between the amide N of Glu317 and O4′ (Table 4). In the
UDP-gal complex, additional hydrogen bonds with O2′ are
formed by the peptide O of Ala282 and with O3′ by the
peptide N of Ala 281 and a water molecule; also, H-bonds
to O5′ and O6′ of the galactose moiety and O1B of the
β-phosphate of UDP are provided by a second water

molecule that is also close to the C1′ carbon (3.87 Å). The
difference in interactions between enzyme and substrate,
relative to inhibitor, does not appear to be associated directly
with structural differences between the Arg365Lys and
Glu317Gln mutants themselves since Arg or Lys365 does
not interact with the hexose and the interaction of Glu/Gln317
with hexose is unchanged in the complex. Instead, the subtle
differences in interactions between the substrate relative to
its inhibitory analogue may be important for reducing the
free energy barrier between the ternary enzyme−substrate
complex and transition state as opposed to formation of a
stable enzyme−inhibitor complex. The previously character-
ized enzyme−product complex of the UDP-gal hydrolysis
reaction contains β-galactose as well as UDP, suggesting that
galactose transfer to water is an inverting reaction. The ability
of α3GT to transfer to small molecules with inversion of
configuration was confirmed by Monegal and Planas (*31*),
who showed that the extremely low hydrolase activity of
the α3GT Glu317Ala mutant can be partially "rescued" by
azide to produce β-galactosylazide. Rescue by azide did not
occur with the Glu317Gln mutant used in the present study,
suggesting that the binding of azide is blocked by the larger
glutamine side chain (*31*).

The effects of substitutions on steady-state kinetic param-
eters (Table 3) clarify the contributions of α3GT interactions
with the α-galactosyl moiety of the donor substrate to
catalysis and substrate binding. The negative charge on
Asp316 is crucial for activity since the Asn mutant has
insignificant catalytic activity, but the Glu mutant has a high
level of activity with a k_{cat} that is 2.5-fold lower than wild-
type but an ∼4-fold lower K_m for acceptor substrate resulting
in a catalytic efficiency ($k_{cat}/K_{ia}K_b$) that is similar to the wild-
type enzyme. The structures of these mutants show that the
inactivating Asn mutation does not disrupt the overall
structure of α3GT but has a localized effect on the structure
of the active site. In wild-type α3GT, the side-chain carboxyl
group of Asp316 interacts with the NH2 of Arg202. In the
Asn mutant, the loss of the negative charge appears to disrupt
this interaction resulting in a 180° rotation of the Asn side
chain. It appears that this prevents its interaction with the
galactose O4′ and may also perturb the interaction between
Arg202 and O3′ of the galactose. A model of UDP-gal
complexed with the crystal structure of the Asp316Asn
mutant showed that the Asn residue faces away from the
galactose moiety and, unless there is a significant substrate-
induced conformational change, will be unable to interact
with the galactose. Therefore, it is reasonable to conclude
that the lack of activity in this mutant reflects a change in
the binding of the donor substrate that disrupts progress
toward the transition state for galactose transfer. While
His315 interacts with O6′ of the galactose, it can be mutated
to Ala with relatively minor effects on activity, suggesting
that this interaction is not important for catalysis. These
results are consonant with a previous study in which a series
of deoxy analogues of UDP-gal were evaluated as substrates
of α3GT and two other galactosyltransferases; the results
indicated that interactions with the 3-, 4-, and 6-OH groups
are important for catalysis by α3GT, the strongest effect
being associated with the 3-OH and weakest with 6-OH (*32*).
Very recently, the structure has been reported for the complex
of a mutant of blood group B glycosyltransferase with UDP-
gal and an acceptor substrate analogue inhibitor (*33*). In this

structure, the conformation of the bound UDP-gal is similar to that described here for the α3GT complex, and the interactions between the enzyme and the galactosyl moiety are also similar to those identified here. Two differences are (i) the only H-bond interaction with the 2′-OH group is through the side chain of Asp211, which corresponds to Asp225 of α3GT; the residue corresponding to His280 is Met in this construct which does not interact with the 2′-OH; (ii) there is no equivalent to the water molecule that H-bonds with O5′ and O6′ in α3GT. This suggests that this solvent molecule is either a unique feature of the α3GT complex or is stabilized in this location by crystal packing.

A crystal structure of α3GT in a complex containing both the donor and acceptor substrates or inhibitory analogues thereof is not currently available. However, the availability of the UDP-gal complex allows us to generate a model of this complex by adding to the Glu317Gln-UDP-gal complex structure an *N*-acetyllactosamine molecule in an orientation and location corresponding to that in the complex of wild-type α3GT with UDP and *N*-acetyllactosamine (PDB code 1GX4 (*15*)). This modeled ternary complex is devoid of clashes between substrates or between substrates and enzyme, consistent with the ordered sequential nature of the catalytic mechanism of α3GT (*15, 19*). In this model, the hydroxyl O3 atom from the galactose moiety of *N*-acetyllactosamine is 2.5 Å from the anomeric carbon C1′ of UDP-gal, but no other polar atoms are within 4 Å of the reactive center C1′. This appears to be inconsistent with a double displacement mechanism that has a *β*-galactosyl-enzyme covalent intermediate and suggests that the acceptor substrate is a viable candidate as the nucleophile in an internal nucleophilic substitution (S_Ni) mechanism (Figure 2B). Glu317 which has been previously proposed as the catalytic nucleophile in a double displacement mechanism (*25*) is positioned on the *β*-face of the galactose moiety but is too distant from the C1′ carbon (4.8 Å) to act as a nucleophile in this type of mechanism, unless there is a major conformational change that allows a close approach of residue 317 to C1′ in the ternary enzyme complex.

ACKNOWLEDGMENT

REFERENCES

1. Varki, A. (1993) Biological roles of oligosaccharides: all of the theories are correct. *Glycobiology 3*, 97–130.

2. Ohtsubo, K., and Marth, J. D. (2006) Glycosylation in cellular mechanisms of health and disease. *Cell 126*, 855–867.

3. Karlsson, K. A. (2001) Pathogen-host protein-carbohydrate interactions as the basis of important infections. *Adv. Exp. Med. Biol. 491*, 431–443.

4. Muramatsu, T. (2000) Protein-bound carbohydrates on cell-surface as targets of recognition: an odyssey in understanding them. *Glycoconjugate J. 17*, 577–595.

5. Breton, C., Snajdrova, L., Jeanneau, C., Koca, J., and Imberty, A. (2006) Structures and mechanisms of glycosyltransferases. *Glycobiology 16*, 29R–37R.

6. Campbell, J. A., Davies, G. J., Bulone, V., and Henrissat, B. (1997) A classification of nucleotide-diphospho-sugar glycosyltransferases based on amino acid sequence similarities. *Biochem. J. 326*, 929–939.

7. Coutinho, P. M., Deleury, E., Davies, G. J., and Henrissat, B. (2003) An evolving hierarchical family classification for glycosyltransferases. *J. Mol. Biol. 328*, 307–317.

8. Galili, U., Shohet, S. B., Kobrin, E., Stults, C. L., and Macher, B. A. (1988) Man, apes, and Old World monkeys differ from other mammals in the expression of alpha-galactosyl epitopes on nucleated cells. *J. Biol. Chem. 263*, 17755–17762.

9. Galili, U., and Swanson, K. (1991) Gene sequences suggest inactivation of alpha-1,3-galactosyltransferase in catarrhines after the divergence of apes from monkeys. *Proc. Natl. Acad. Sci. U.S.A. 88*, 7401–7404.

10. Takeuchi, Y., Porter, C. D., Strahan, K. M., Preece, A. F., Gustafsson, K., Cosset, F. L., Weiss, R. A., and Collins, M. K. (1996) Sensitization of cells and retroviruses to human serum by (alpha 1−3) galactosyltransferase. *Nature 379*, 85–88.

11. Joziasse, D. H., and Oriol, R. (1999) Xenotransplantation: the importance of the Galalpha1,3Gal epitope in hyperacute vascular rejection. *Biochim. Biophys. Acta 1455*, 403–418.

12. Kuwaki, K., Tseng, Y. L., Dor, F. J., Shimizu, A., Houser, S. L., Sanderson, T. M., Lancos, C. J., Prabharasuth, D. D., Cheng, J., Moran, K., Hisashi, Y., Mueller, N., Yamada, K., Greenstein, J. L., Hawley, R. J., Patience, C., Awwad, M., Fishman, J. A., Robson, S. C., Schuurman, H. J., Sachs, D. H., and Cooper, D. K. (2005) Heart transplantation in baboons using alpha1,3-galactosyltransferase gene-knockout pigs as donors: initial experience. *Nat. Med. 11*, 29–31.

13. Yamada, K., Yazawa, K., Shimizu, A., Iwanaga, T., Hisashi, Y., Nuhn, M., O'Malley, P., Nobori, S., Vagefi, P. A., Patience, C., Fishman, J., Cooper, D. K., Hawley, R. J., Greenstein, J., Schuurman, H. J., Awwad, M., Sykes, M., and Sachs, D. H. (2005) Marked prolongation of porcine renal xenograft survival in baboons through the use of alpha1,3-galactosyltransferase gene-knockout donors and the cotransplantation of vascularized thymic tissue. *Nat. Med. 11*, 32–34.

14. Boix, E., Swaminathan, G. J., Zhang, Y., Natesh, R., Brew, K., and Acharya, K. R. (2001) Structure of UDP complex of UDP-galactose:beta-galactoside-alpha-1,3-galactosyltransferase at 1.53-Å resolution reveals a conformational change in the catalytically important C terminus. *J. Biol. Chem. 276*, 48608–48614.

15. Boix, E., Zhang, Y., Swaminathan, G. J., Brew, K., and Acharya, K. R. (2002) Structural basis of ordered binding of donor and acceptor substrates to the retaining glycosyltransferase, alpha-1,3-galactosyltransferase. *J. Biol. Chem. 277*, 28310–28318.

16. Zhang, Y., Swaminathan, G. J., Deshpande, A., Boix, E., Natesh, R., Xie, Z., Acharya, K. R., and Brew, K. (2003) Roles of individual enzyme-substrate interactions by alpha-1,3-galactosyltransferase in catalysis and specificity. *Biochemistry 42*, 13512–13521.

17. Zhang, Y., Deshpande, A., Xie, Z., Natesh, R., Acharya, K. R., and Brew, K. (2004) Roles of active site tryptophans in substrate binding and catalysis by alpha-1,3 galactosyltransferase. *Glycobiology 14*, 1295–1302.

18. Jamaluddin, H., Tumbale, P., Withers, S. G., Acharya, K. R., and Brew, K. (2007) Conformational changes induced by binding UDP-2F-galactose to alpha-1,3 galactosyltransferase—implications for catalysis. *J. Mol. Biol. 369*, 1270–1281.

19. Zhang, Y., Wang, P. G., and Brew, K. (2001) Specificity and mechanism of metal ion activation in UDP-galactose:beta-galactoside-alpha-1,3-galactosyltransferase. *J. Biol. Chem. 276*, 11567–11574.

20. Otwinowski, Z., and Minor, W. (1997) Processing of X-ray diffraction data collected in oscillation mode. *Methods Enzymol. 276*, 307–326.

21. Vagin, A., and Teplyakov, A. (1997) MOLREP: an automated program for molecular replacement. *J. Appl. Crystallogr. 30*, 1022–1025.

22. Brünger, A. T., Adams, P. D., Clore, G. M., DeLano, W. L., Gros, P., Grosse-Kunstleve, R. W., Jiang, J. S., Kuszewski, J., Nilges, M., Pannu, N. S., Read, R. J., Rice, L. M., Simonson, T., and Warren, G. L. (1998) Crystallography & NMR system: A new software suite for macromolecular structure determination. *Acta Crystallogr. D 54*, 905–921.

23. Project, C. C. (1994) The CCP4 suite: programs for protein crystallography. *Acta Crystallogr. D 50*, 760–763.

24. Emsley, P., and Cowtan, K. (2004) Coot: model-building tools for molecular graphics. *Acta Crystallogr. D 60*, 2126–2132.

25. Gastinel, L. N., Bignon, C., Misra, A. K., Hindsgaul, O., Shaper, J. H., and Joziasse, D. H. (2001) Bovine alpha1,3-galactosyltransferase catalytic domain structure and its relationship with ABO

histo-blood group and glycosphingolipid glycosyltransferases. *EMBO J. 20*, 638–649.

26. Persson, K., Ly, H. D., Dieckelmann, M., Wakarchuk, W. W., Withers, S. G., and Strynadka, N. C. (2001) Crystal structure of the retaining galactosyltransferase LgtC from *Neisseria meningitidis* in complex with donor and acceptor sugar analogs. *Nat. Struct. Biol. 8*, 166–175.

27. Brayer, G. D., Sidhu, G., Maurus, R., Rydberg, E. H., Braun, C., Wang, Y., Nguyen, N. T., Overall, C. M., and Withers, S. G. (2000) Subsite mapping of the human pancreatic alpha-amylase active site through structural, kinetic, and mutagenesis techniques. *Biochemistry 39*, 4778–4791.

28. Xu, H., Storch, T., Yu, M., Elliott, S. P., and Haslam, D. B. (1999) Characterization of the human Forssman synthetase gene. An evolving association between glycolipid synthesis and host-microbial interactions. *J. Biol. Chem. 274*, 29390–29398.

29. Martinez-Fleites, C., Proctor, M., Roberts, S., Bolam, D. N., Gilbert, H. J., and Davies, G. J. (2006) Insights into the synthesis of lipopolysaccharide and antibiotics through the structures of two retaining glycosyltransferases from family GT4. *Chem. Biol. 13*, 1143–1152.

30. Angulo, J., Langpap, B., Blume, A., Biet, T., Meyer, B., Krishna, N. R., Peters, H., Palcic, M. M., and Peters, T. (2006) Blood group B galactosyltransferase: insights into substrate binding from NMR experiments. *J. Am. Chem. Soc. 128*, 13529–13538.

31. Monegal, A., and Planas, A. (2006) Chemical rescue of alpha3-galactosyltransferase. Implications in the mechanism of retaining glycosyltransferases. *J. Am. Chem. Soc. 128*, 16030–16031.

32. Sujino, K., Uchiyama, T., Hindsgaul, O., Seto, N. O. L., Wakarchuk, W. W., and Palcic, M. M. (2000) Enzymatic synthesis of oligosaccharide analogues: evaluation of UDP-gal analogues as donors for three retaining galactosyltransferases. *J. Am. Chem. Soc. 122*, 1261–1269.

33. Alfaro, J. A., Zheng, R. B., Persson, M., Letts, J. A., Polakowski, R., Bai, Y., Borisova, S. N., Seto, N. O., Lowary, T. L., Palcic, M. M., and Evans, S. V. (2008) ABO(H) blood group A and B glycosyltransferases recognize substrate via specific conformational changes. *J. Biol. Chem. 283*, 10097–10108.

34. Esnouf, R. M. (1997) An extensively modified version of MolScript that includes greatly enhanced coloring capabilities. *J. Mol. Graphics Modell. 15*, 132–134.